Nuclear Instruments and Methods in Physics Research A 822 (2016) 9–14

Contents lists available at ScienceDirect

Nuclear Instruments and Methods in Physics Research A

journal homepage: www.elsevier.com/locate/nima

Response functions of semiconducting lithium indium diselenide

Eric Lukosi [a,*], Ondrej Chvala [a], Ashley Stowe [a,b]

[a] University of Tennessee, Knoxville, TN, USA
[b] Y-12 National Security Complex, Oak Ridge, TN, USA

ARTICLE INFO

Article history:
Received 16 December 2015
Received in revised form
24 March 2016
Accepted 24 March 2016
Available online 25 March 2016

Keywords:
Lithium indium diselenide
LISe
Neutron/gamma discrimination
Neutron detection
Neutron semiconductor detector
Charge collection efficiency

ABSTRACT

This paper presents the results of a computational investigation that determined the gamma-ray and neutron response functions of a new semiconducting material, $^{6}LiInSe_2$, which is very sensitive to thermal neutrons. Both MCNP6 simulations and custom post-processing/simulation techniques were used to determine various detection properties of LISe. The computational study included consideration of energetic electron escape, the contribution from the activation of ^{115}In and subsequent decay of ^{116}In, triton and alpha particle escape from the ^{6}Li reaction pathway, and the effect of incomplete charge collection when detecting neutrons via the ^{6}Li reaction pathway. The result of neutron detection with incomplete charge collection was compared to experimental results and showed general agreement, where holes exhibit a lower mobility-lifetime product than electrons, as expected for compound semiconductors.

1. Introduction

One goal in the radiation detection community is the development of a direct, thermal neutron detection system that relies on the direct sensing of charge created by the products of a neutron reaction. For gaseous detectors, this was achieved many decades ago using ^{3}He and $^{10}BF_3$ fill gasses. For solid state devices, both conversion layers and semiconductors containing a neutron-sensitive isotope have been investigated [1]. For instance, the research group lead by McGregor [2,3] have invested considerable time on microstructured semiconductor neutron detectors (MSNDs), where the trenches are filled with either a ^{10}B or ^{6}Li containing material. They have demonstrated detection efficiencies for thermal neutrons of 32% using a two detector stack design (16% per silicon substrate). Direct detection semiconductors [4], such as boron carbide [5,6], boron phosphide [7,8], and boron nitride [9–11], have also been investigated for some time. Boron carbide and boron nitride have shown response to neutrons, but to the knowledge of this author, boron phosphide has yet to demonstrate a neutron response in published literature. Still, all three of these detectors are limited in performance because of growth challenges affecting usable detection volumes, poor charge collection efficiency, and/or inadequate neutron/gamma discrimination. Therefore, while the literature indicates the potential of these three boron containing semiconductors, their performance and technology readiness level have not yet reached a level suitable for commercialization.

In recent literature [12,13], a new semiconductor, lithium indium diselenide ($^{6}LiInSe_2$ or LISe), has demonstrated direct neutron detection through the collection of generated electron–hole pairs. The spectrum obtained is a continuous distribution, although peaks are observed via alpha exposures when collecting electrons [13]. This indicates that the charge carrier properties of holes is poor, which is common for tertiary compound semiconductors [4]. It should also be noted that LISe has demonstrated scintillation response to radiation as well [14,15], but is not the focus of this paper.

For thermal neutrons, every isotope within LISe has a measurable absorption cross section, but the response is dominated by the $^{6}Li(n,^{3}H)^{4}He$ and $^{115}In(n,\gamma)^{116}In$ reactions, which have thermal neutron cross sections of 938 b and 202 b, respectively. The specifics of the latter reaction can be found in [15]. The beta particles and gamma-rays that are emitted as a result of neutron capture by ^{115}In may deposit energy within LISe, resulting in signal formation. The direct measurement of the decay of ^{115}In from thermal neutron activation has recently been reported in the literature [16], where the number of counts vs time was reported. The cross section of LISe, ^{6}Li in LISe, and the scattering cross section of ^{6}Li in LISe is shown in Fig. 1.

As the development of LISe continues, a question that remains is the expected response of LISe to neutrons and gamma-rays. This paper reports on the expected differential pulse height spectrum (DPHS) of LISe in a variety of circumstances. This paper reports on the response of LISe to gamma-rays with ideal charge collection

* Corresponding author.

http://dx.doi.org/10.1016/j.nima.2016.03.080
0168-9002/

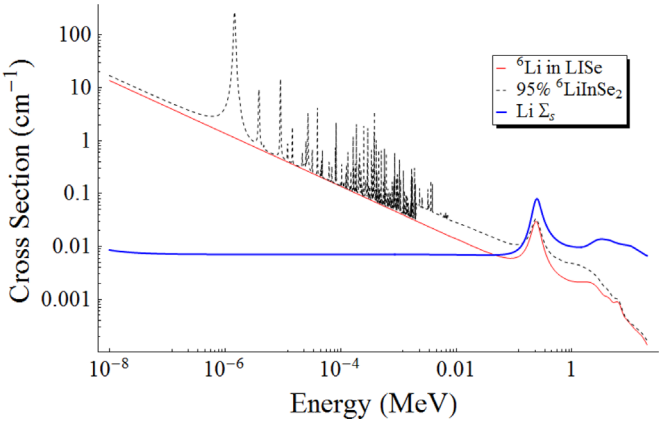

Fig. 1. Neutron absorption cross section of LISe and ^{6}Li in LISe as well as neutron elastic scattering with ^{6}Li [17]. Cross section data was obtained from the NNDC Database, library ENDF/B-VII.1.

properties, where consideration of the peak-to-total and range of energetic electrons within LISe is given. Also reported is the expected DPHS when prompt and delayed gamma-ray production and secondary charged particle escape from neutron reactions are considered. Finally, the effect of charge collection on the DPHS is investigated for the primary ^{6}Li(n,^{3}H)^{4}He reaction of interest.

2. Methodology

MCNP6 [17] was used to simulate the DPHS of LISe from thermal neutrons and gamma-rays under ideal charge collection using the F8 tally. The NCIA algorithm and the PHL modifier was used to correlate secondary charged particles. The ACT card was utilized to simulate the decay of activated isotopes, important for ^{115}In activation. The DPHS generated from gamma-rays is dependent on the transport of electrons in LISe. As such, the range of electrons in LISe provides a measure of the expected electron escape from the crystal bulk as a function of energy. The photoelectric response of LISe is therefore a function of LISe geometry, interaction location, and electron energy. Energetic electron range as a function of energy was determined via the stopping power tables from MCNP6, the ESTAR database [18], and direct transport of a pencil beam of beta particles striking a large planar LISe surface in MCNP6 to determine at what depth the electron population above 1 keV drops below 0.5%. The latter of the three was chosen because the default electron energy when transport is terminated in MCNP6 is 1 keV, and a cutoff of 0.5% of the incident electron population represents the depth when the electron population is too low to significantly contribute to a measured response in LISe.

To consider the effect of incomplete charge collection, the range of the secondary charged particles play a critical role. The range and Bragg curves were determined using SRIM [19]. It was found that the range of the triton and alpha particle from the ^{6}Li (n,^{3}H)^{4}He reaction in LISe was 39.4 μm and 7.44 μm, respectively. These ranges are not insignificant for detector thicknesses yielding near maximum thermal neutron absorption efficiency (~65% neutron absorption efficiency at 0.1 cm) [15]. Consequently, a simple mesh geometry is not suitable to construct accurate DPHS, as reported in [20], so a custom program was written using ROOT/C++ framework [21] to take into account charge trapping.

The custom program used first order transport theory to estimate the reaction rate of neutrons within a differential distance of LISe from a plane wave of impinging thermal neutrons on the cathode. At each differential position, the emission angle, defining the velocity vector, of the alpha particle and triton was sampled uniformly. These two particles are emitted anti-parallel for thermal neutrons. We assume a 2π symmetry in a planar geometry with no field fringing (semi-infinite geometry). Then, the Bragg curves simulated in SRIM for each particle are superimposed on its corresponding velocity vector, and the energy deposited in user-defined spatial bins along the electric field vector is determined through projection of the integral of the Bragg curve in each spatial bin. The units are kept in energy because the W-value of LISe has yet to be accurately determined. The number of electrons and holes collected at their respective electrodes are simulated through applying a summation of Hecht's equation to each bin, as defined in Eq. (1).

$$Q = \sum_{i=1}^{N} Q_{o,i}\left\{\frac{\mu_e\tau_e E}{d}\left(1-\mathrm{Exp}\left[\frac{-x_i}{\mu_e\tau_e E}\right]\right)+\frac{\mu_h\tau_h E}{d}\left(1-\mathrm{Exp}\left[\frac{-(d-x_i)}{\mu_h\tau_h E}\right]\right)\right\} \quad (1)$$

In Eq. (1), Q is the total collected signal, $Q_{o,i}$ is the generated signal in spatial bin i, $\mu_{e/h}$ is the mobility of electrons/holes, $\tau_{e/h}$ is the trapping time constant of electrons/holes, E is the electric field applied across the sensor, x_i is the average position in each spatial bin, and d is the thickness of the sensor in the direction of charge collection. In this model, the geometry is assumed semi-infinite (parallel plate capacitor) with no polarization, surface recombination, sensor electronic property inhomogeneity, or charge carrier detrapping within the sensitive timeframe of the processing electronics. The ratio of Q-to-Q_o yields the charge collection efficiency of the device (note that energy can be easily converted to charge through the W-value, and cancels out, such that the result is the same). A pictorial representation of the described simulation methodology is provided in Fig. 2. The qualitative representation of the Bragg curves are shown in red and follow the path of the secondary particle (i.e., alpha or tritium particle). The energy deposited in each region, x_i defines $Q_{o,i}$, and then Eq. (1) is used to construct the expected DPHS.

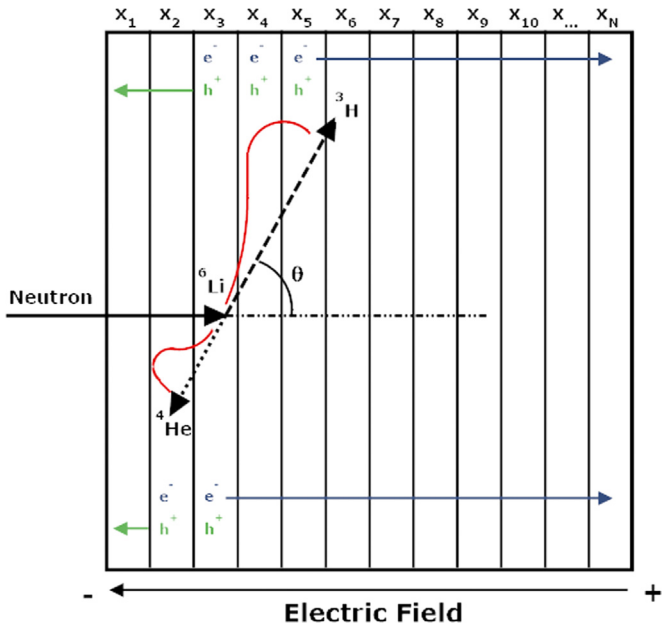

Fig. 2. Pictorial representation of simulation methodology for first order response of ^{6}LiInSe2 crystal to thermal neutrons. The red lines represent a qualitative representation of the Bragg curves for triton and alpha particle emitted. (For interpretation of the references to color in this figure legend, the reader is referred to the web version of this article.)